



Research Paper

Nicotinamide nucleotide transhydrogenase-mediated redox homeostasis promotes tumor growth and metastasis in gastric cancer

Shuai Li^{a,1}, Zhuonan Zhuang^{b,1}, Teng Wu^a, Jie-Chun Lin^a, Ze-Xian Liu^c, Li-Fen Zhou^a, Ting Dai^a, Lei Lu^a, Huai-Qiang Ju^{c,*}

^a Department of Biochemistry and Molecular Biology, GMU-GIBH Joint School of Life Sciences, Guangzhou Medical University, Guangzhou 510182, PR China

^b Department of Gastrointestinal Surgery, Beijing Tsinghua Changgung Hospital Medical Center, Tsinghua University, Beijing 102218, China

^c Sun Yat-sen University Cancer Center, State Key Laboratory of Oncology in South China, Collaborative Innovation Center for Cancer Medicine, Guangzhou 510060, China



ARTICLE INFO

Keywords:

NNT
Gastric cancer
NADPH
Anoikis resistance
Metastasis

ABSTRACT

Overcoming oxidative stress is a critical step for tumor growth and metastasis, however the underlying mechanisms in gastric cancer remain unclear. In this study, we found that overexpression of nicotinamide nucleotide transhydrogenase (NNT) was associated with shorter overall and disease free survival in gastric cancer. The NNT is considered a key antioxidative enzyme based on its ability to regenerate NADPH from NADH. Knockdown of NNT caused significantly NADPH reduction, induced high levels of ROS and significant cell apoptosis under oxidative stress conditions such as glucose deprivation and anoikis. *In vivo* experiments showed that NNT promoted tumor growth, lung metastasis and peritoneal dissemination of gastric cancer. Moreover, intratumoral injection of NNT siRNA significantly suppressed gastric tumor growth in patient-derived xenograft (PDX) models. Overall, our study highlights the crucial functional roles of NNT in redox regulation and tumor progression and thus raises an important therapeutic hypothesis in gastric cancer.

1. Introduction

Gastric cancer (GC) is the most common gastrointestinal neoplasm and is a leading cause of cancer-related deaths worldwide [1–3]. The high growth ability and mortality rate of GC is evident as it spreads to distant organs; for example, peritoneal dissemination is a common development in patients with advanced GC even at initial diagnosis and carries a very poor prognosis [4]. However, its molecular mechanism has not been clear elucidated. Growing evidence points to the fundamental role of redox homeostasis in tumorigenesis and metastatic progression [5–7]. Yet, the regulation of NADPH metabolism in GC remains unclear.

In cancer cells, overcoming oxidative stress is a critical step for tumor progression. Redox homeostasis is dependent on a balance between the levels of antioxidants such as NADPH, used to maintain reduced glutathione (GSH), and oxidants such as reactive oxygen species (ROS). During tumor progression, cancer cells usually suffer from oxidative stress caused by ischemia, hypoxia and anchorage-independent

growth when tumor growth exceeds the ability of available vasculature to supply tumor cells with oxygen [8–10]. Though ROS are essential for adequate signal transduction and are known to regulate crucial cellular processes. However, once the balance is broken, rapid increases in intracellular ROS may lead to cell apoptosis, and cells frequently demand for more NADPH to eliminate excess ROS.

NNT is considered a key antioxidative enzyme based on its ability to regenerate NADPH from NADH and is the major mitochondrial enzymatic source of NADPH, contributing 45% of the total NADPH supply [11]. NNT is at the critical interface between the NADH and NADPH pools in mitochondria; the NNT catalyzes the reaction $\text{NADH} + \text{NADP}^+ \leftrightarrow \text{NADPH} + \text{NAD}^+$ [12]. Recently, our studies shows that disrupting G6PD- or ME2-mediated NADPH homeostasis enhances chemosensitivity in gastrointestinal cancer [13,14]. In humans and animals, NNT dysfunction usually leads to oxidative stress [15–17]. However, the effects of NNT on NADPH homeostasis and tumor malignant phenotypes in GC remain unclear.

Here, we identified that NNT is overexpressed in GC. Given that

Abbreviations: NNT, nicotinamide nucleotide transhydrogenase; ROS, reactive oxygen species; GC, gastric cancer; NADH, nicotinamide adenine dinucleotide; NADPH, nicotinamide adenine dinucleotide phosphate; Ploy-HEMA, ploy-2-hydroxyethylmethacrylate

* Corresponding author. Address: 651 Dongfeng East Road, Guangzhou 510060, China.

E-mail address: juhq@sysucc.org.cn (H.-Q. Ju).

¹ These authors contributed equally to this work.

<https://doi.org/10.1016/j.redox.2018.07.017>

Received 26 June 2018; Received in revised form 20 July 2018; Accepted 20 July 2018

Available online 21 July 2018

2213-2317/ © 2018 The Authors. Published by Elsevier B.V. This is an open access article under the CC BY-NC-ND license

(<http://creativecommons.org/licenses/by-nc-nd/4.0/>).

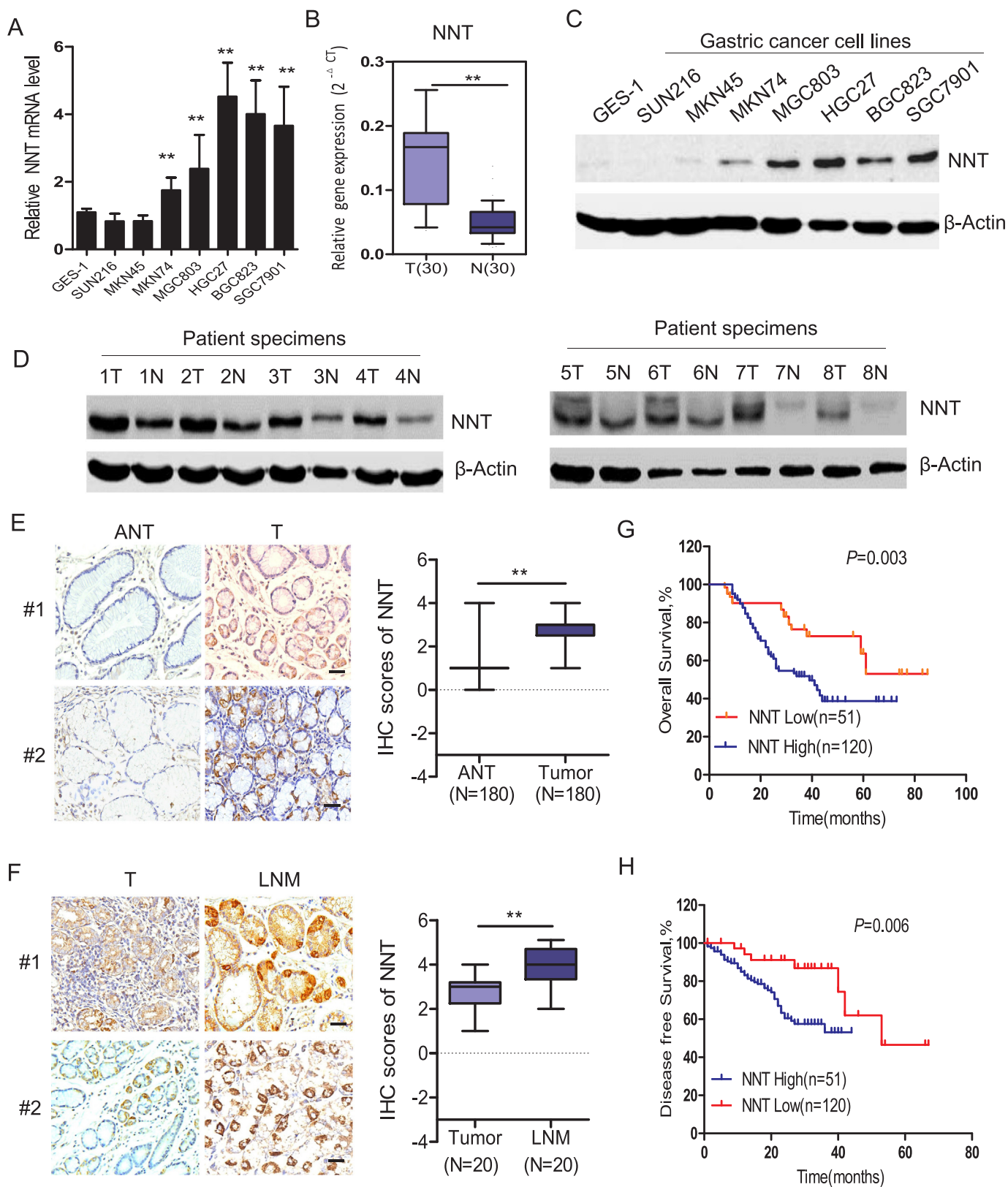


Fig. 1. Increased NNT expression is correlated with poor prognosis in GC. (A) qPCR analysis of NNT expression in a panel of gastric cancer (GC) cells and GES-1 epithelial cells. (B) qPCR analysis of NNT expression in 30 paired GC tissues obtained from our hospital. (C) Immunoblotting analysis of NNT protein levels in a panel of GC cells and GES-1 epithelial cells. (D) Immunoblotting analysis of NNT protein levels in 8 paired GC tissues. (E) Representative staining (left panel) and immunoscore of NNT (right panel, N = 180) showing low expression of NNT protein in adjacent normal tissues (ANT), positive staining in primary GC tumor tissues (scale bar: 100 μm). (F) Representative staining (left panel) and immunoscore of NNT (right panel) in primary GC tumor tissues and paired lymph node metastatic tissues (LNM, N = 20) (scale bar: 100 μm). Kaplan-Meier analysis of overall survival (G) or disease-free survival curves (H) for GC patients with low versus high expression of NNT (Kaplan-Meier analysis with the log-rank test). Data are presented as the mean ± SD. **P < 0.01 for indicated comparison.

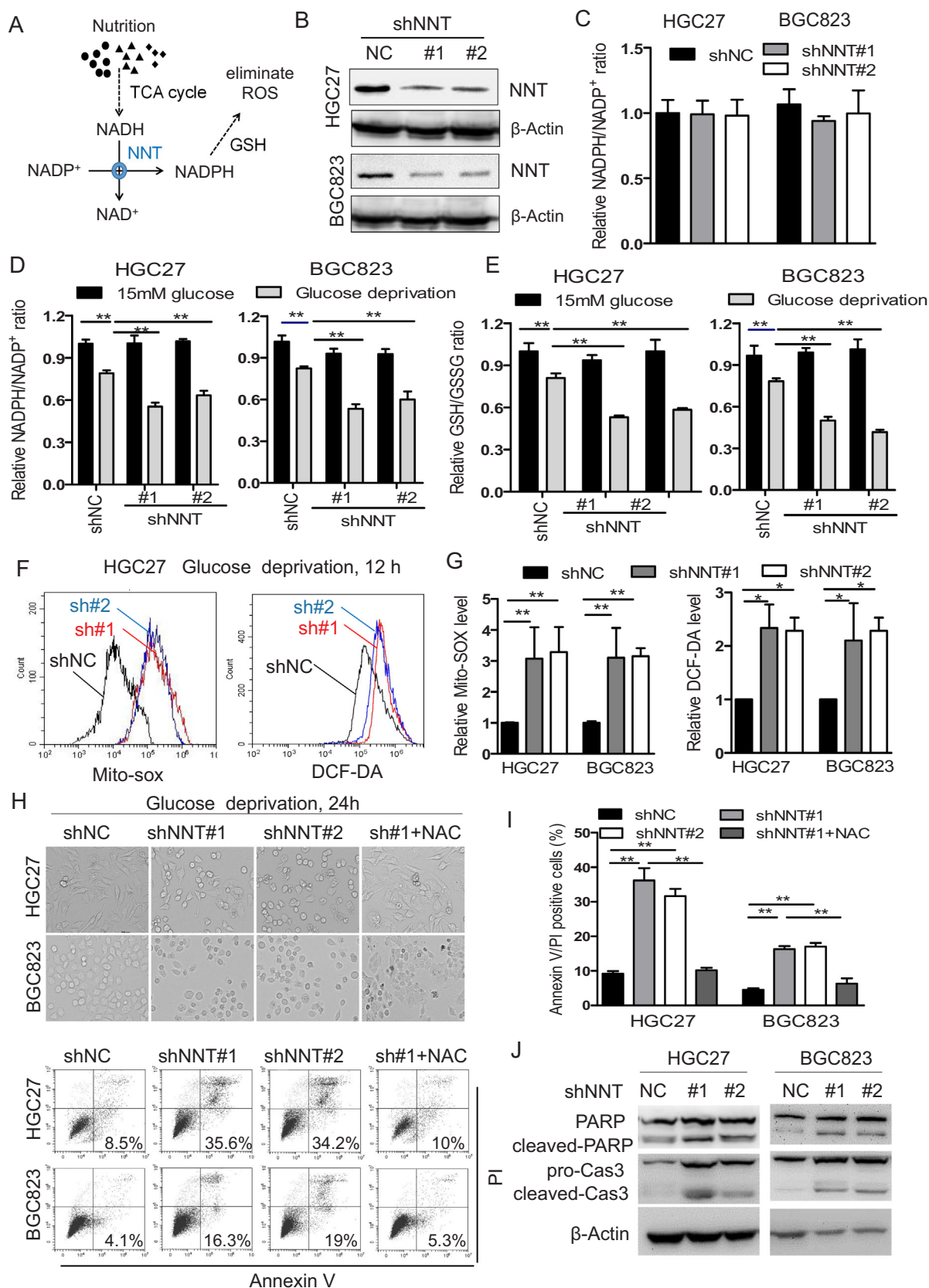


Fig. 2. NNT is essential for cell survival during glucose deprivation. (A) Overview of the relationship between the NNT enzyme reaction and ROS elimination. (B) The effect of NNT-targeting shRNAs in HGC27 and BGC823 cells was confirmed by western blot analysis. (C) Measurement of NADPH/NADP⁺ in the indicated cells cultured in normal medium. (D–E) Measurement of NADPH/NADP⁺ and GSH/GSSG levels in the indicated cells cultured in glucose deprivation medium. (F–G) Representative histograms and quantification of mitochondria ROS and cellular H₂O₂ levels in the indicated GC cells cultured in glucose deprivation medium for 12 h. (H) Bright field images and apoptosis of the indicated cells cultured in glucose deprivation medium. Representative images and quantification data are shown. (J) Immunoblotting analysis of total and cleaved PARP and caspase 3 in the indicated GC cells cultured under glucose starvation. All error bars represent the S.D. of at least three replicates from two independent experiments. ***P* < 0.01 for indicated comparison, *P* values were determined by a two-tailed *t*-test.

glucose starvation or anchorage independence induces ROS generation [10], we hypothesized that NNT-mediated NADPH homeostasis may have the capacity to protect against oxidative stress, resulting in GC progression. Further experiments using NNT-knockdown GC cells revealed that NNT was critical to GC cell growth under oxidative stress. In the present study, we first investigated the crucial functional roles of NNT in redox regulation and tumor progression, thus raising an important therapeutic hypothesis in gastric cancer.

2. Materials and methods

2.1. Cell lines and cell culture

GES-1, SGC7901, SNU216, MKN45, MKN74, BGC823, HGC27 and MGC803 were purchased from ATCC (Manassas, VA, USA) and cultured under conditions specified by the supplier. Glucose-free medium (GIBCO, #11879020) supplemented with 10% dialyzed FBS was used for glucose deprivation assays. The anchorage-independent growth of cells was performed in poly-2-hydroxyethyl methacrylate-coated dishes (poly-HEMA; Sigma, P3932) [18]. Poly-HEMA powder was dissolved to 12 mg/mL in 95% ethanol. All cells tested negative for mycoplasma and were authenticated by short tandem repeat DNA fingerprinting at the Medicine Lab of the Forensic Medicine Department of Sun Yat-sen University (Guangzhou, China).

2.2. Tissue specimens and clinicopathological characteristics

The 180 paraffin-embedded, archived gastric samples used in this study were histopathologically and clinically diagnosed at the Sun Yat-sen University Cancer Center between 2007 and 2009. Written informed consent was obtained from all patients, and no patient received any chemo- or radiotherapy prior to surgery. The use of clinical specimens for research purposes was conducted in accordance with the Declaration of Helsinki and approved by the ethical committee of Sun Yat-sen University Cancer Center. The clinicopathological characteristics of the samples are summarized in [online Supplementary Table S1](#). 171 patients were followed-up regularly after the operation at three-month intervals. Thirty freshly collected gastric cancer tissues and matched adjacent nontumoral gastric tissues were frozen and stored in liquid nitrogen until required for RNA and protein extraction.

2.3. Immunohistochemistry (IHC) and immunoblotting analysis

Immunohistochemical and immunoblotting analyses were conducted according to standard procedures as described previously [13]. DAB substrate was used to detect protein expression, and counterstaining color was carried out using Hematoxylin. The TUNEL assays were performed with the *In Situ* Cell Death Detection Kit (Promega, #G3250) according to the manufacturer's instructions. For immunoblotting analysis, total proteins were extracted with the RIPA lysis buffer, and the protein concentrations were measured using the BCA Protein Assay (Thermo Fisher Scientific, #23225). Equal amounts of cell protein were subjected to electrophoresis in SDS-PAGE gels and then transferred to PVDF membranes (Millipore) for antibody blotting. Antibodies used in our study were as follows: NNT (Proteintech, #13442-2-AP), Ki-67 (CST, #9129), PARP (CST, #9532), caspase 3 (CST, #9662), and β -Actin (CST, #4970).

2.4. RNA extraction and qRT-PCR analysis

Total RNA was isolated from cells or tissues by TRIzol reagent (Invitrogen). Total RNA (500 ng) was used for reverse transcription with an iScript cDNA Synthesis Kit (Bio-Rad). The resulting complementary DNA was analyzed by qPCR performed with SYBR reagent using the IQ5 PCR system (Bio-Rad). β -Actin expression was used for normalization. The sequences of the primers used were as follows: NNT

(forward: 5'-tggcaagcagggttttaagt-3', reverse: 5'-tcctttgcccttgattgg-3), β -Actin (forward: 5'-gcactcttcagcttctt-3', reverse: 5'-gttgcgta-caggtctttgc-3).

2.5. RNAi assay and lentiviral transduction

The siRNAs targeting NNT were purchased from RiboBio (Guangzhou, China). Short hairpin RNAs (shRNAs) directed against NNT (#1: TCGTTATCACTGTGCTGAA; #2: CTATGGTTAATCCAACATT) were ligated into the GV112 virus vector (GeneChem, Shanghai, China). The infected cells were selected with 5 μ g/mL puromycin (Sigma-Aldrich, USA).

2.6. ROS and measurement of NADPH

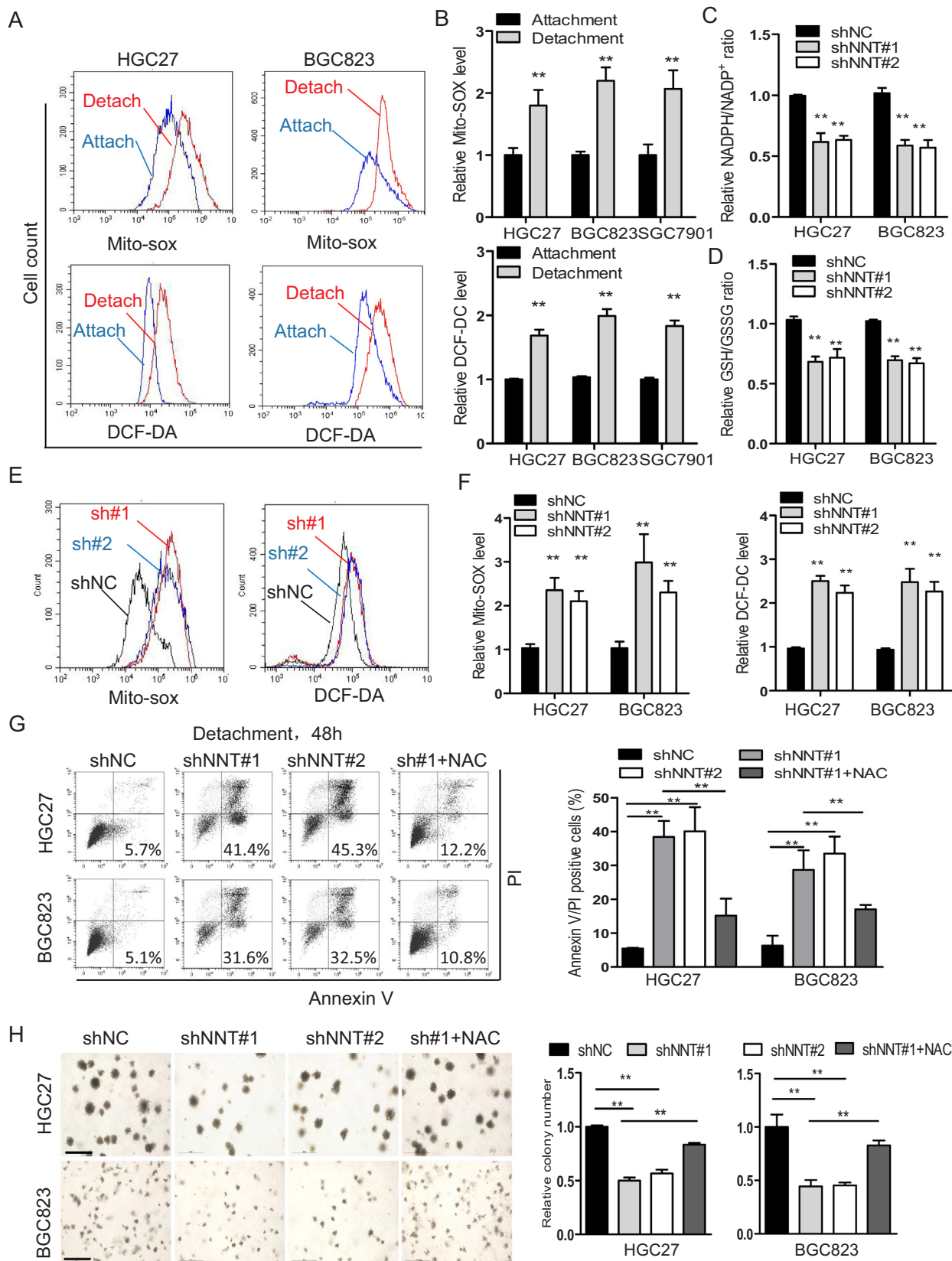
ROS levels were determined as described previously [16,18]. Briefly, cells were incubated with 10 μ M H₂-DCFDA or 5 μ M Mito-SOX at 37 °C for 30 min. Then, the cells were collected and re-suspended in PBS. Fluorescence was immediately measured using a Flow Cytometer (Beckman). *N*-acetyl-L-cysteine (NAC), DCF-DA and Mito-SOX were purchased from Life Technologies (Invitrogen, California, USA) and dissolved in sterile water or DMSO. For the rescue experiment, NAC (1 mM) was used for pretreatment for 3 h before gastric cells under glucose deprivation or detachment conditions, and continued to incubate with the cell lines for 24 h and 48 h, respectively. Intracellular levels of NADPH, total NADP and GSH were measured by the NADP/NADPH-Glo kit (Promega, #G9081) or GSH/GSSG-Glo kit (Promega, #V6612) according to the manufacturer's instructions.

2.7. Apoptosis analysis and soft agar colony formation assay

Anoikis was induced by plating cells on poly-HEMA six-well plates (Sigma, #P3932) as described [16]. For apoptosis analysis, cells were collected and stained with Annexin V-FITC and propidium iodide (PI) (KeyGEN, #KGA108) before measurement using flow cytometer. For the soft agar colony formation assay, equal cell suspension was mixed with 0.7% soft agar dissolved in RPMI 1640 (10% FBS) and layered in triplicate onto 0.7% (RPMI 1640, 10% FBS) solidified agar. After 14 days of culture, colonies were counted under a microscope and photographed.

2.8. Animal experiments

All animal experiments were carried out in accordance with the National Institutes of Health's Guide for the Care and Use of Laboratory Animals with the approval from the Institutional Animal Care and Use Committee of Sun Yat-Sen University. Female athymic mice (4–5 weeks old) were obtained from the Guangdong Province Laboratory Animal Center (Guangzhou, China). The NNT knockdown and control GC cells (2×10^6) were subcutaneously injected into the flanks of the mice (5 mice/group). Every four days after injection, tumor sizes were measured. The PDX-bearing male nude mouse model was raised and passaged as previously described [13,19]. In brief, patient-derived tumor materials were collected in culture medium and necrotic and supporting tissues were carefully removed and transferred to the animal houses on wet ice within 1 h after resection. The tumor gross was cut into different fragments for implanted subcutaneously into the flank region of female nude mice and the incision was closed with surgical suture. Successfully engrafted tumor models were then passaged and used for experiment. When the PDX tumor had grown to an appropriate volume, the tumor-bearing mice were randomly assigned to two groups (5 mice/group), and 10 OD cholesterol-modified NNT siRNA or control siRNA (Ribobio) was intratumorally injected every 4 days for 4 weeks. Tumor size was measured every four days using a caliper, and tumor volume was calculated using the standard formula $V = \text{length} \times \text{width}^2 / 2$.



(caption on next page)

To evaluate the effect of NNT on *in vivo* metastasis, two xenograft models were used. For the lung metastasis model, NNT knockdown and control GC cells (2×10^6) resuspended in 200 μ l of PBS were injected into the tail veins of nude mice (5 mice/group). Lung colonization was

monitored with an imaging system as previously described [13]. Mice were sacrificed with cervical dislocation, the lungs were dissected out, and paraffin was embedded to histopathologically examine the metastatic locus as described previously [20]. The peritoneal dissemination

Fig. 3. NNT suppression accelerates GC anoikis. (A–B) Representative histograms of the quantification of cellular ROS levels in the indicated GC cells under attached or detached conditions for 12 h as detected by the fluorescent probe Mito-SOX and DCF-DA. (C) The NADP/NADP⁺ levels were measured in the indicated GC cells after plating in adherent or poly-HEMA-coated detachment plates for 24 h. (D) Cellular GSH/GSSG levels were measured in the indicated GC cells after plating in adherent or poly-HEMA-coated detachment plates for 24 h. (E–F) Mitochondrial ROS and intracellular ROS levels in HGC27 and BGC823 cells cultured in detached conditions were measured after knockdown of NNT. Representative images and quantification data are shown. (G) Representative histograms depicting apoptosis and the apoptotic rate of indicated cells after 48 h of suspension as determined by flow cytometry. (H) Soft agar colony formation assays in HGC27 and BGC823 cells after knockdown of NNT (scale bar: 500 μm). All error bars represent the S.D. of at least three replicates from two independent experiments. *P* values were determined by a two-tailed *t*-test.

ability of gastric cancer cells was evaluated through intraperitoneal injection. In brief, NNT knockdown and control GC cells (3×10^6) in 400 μl of PBS were injected into the peritoneal cavity. Peritoneum metastasis (6 mice/group) was examined and recorded when mice were killed at 30 days after injection, or for survival analysis, animal survival (10 mice/group) time was recorded.

2.9. Statistical analysis

For error bars in all experiments, standard deviation (s.d.) was calculated from three independent experiments, and values represent the mean \pm s.d. For statistical differences among more than two groups, one-way ANOVA and the Newman Keul's multiple comparison test were used. All other differences were evaluated by Student's unpaired *t*-test. A Kaplan-Meier survival analysis and a log-rank test were used for survival analysis. Differences reached statistical significance with *P* < 0.05 (*) and *P* < 0.01 (**). Statistical computations were performed using Prism software (Graph Pad, La Jolla, CA).

3. Results

3.1. Increased NNT expression is correlated with GC metastasis and poor prognosis

To investigate the expression of NNT in GC, we first analyzed the pattern of NNT expression in a GC cell line and tumor tissue samples isolated from patients with GC. PCR analysis showed that NNT mRNA levels were significantly increased in most detected GC cell lines or GC tissues (T) compared with the nontumorigenic cells (GES1) or adjacent noncancerous tissues (N) (Fig. 1A and B). Immunoblotting analysis showed the NNT protein levels were notably increased in most detected GC cell lines (Fig. 1C). Also, the NNT protein level was notably increased in eight representative GC tissues compared with adjacent noncancerous tissues (Fig. 1D). To investigate the clinical relevance, we then analyzed NNT expression in 180 archived gastric cancer tissues by immunohistochemical (IHC) staining. Consistent with the data obtained from GC cell lines, IHC staining indicated that primary GC tissues (T) had greater NNT expression compared with adjacent normal tissues (ANT) (Fig. 1E). Additionally, NNT expression levels were also significantly increased in lymph node metastasis tissues (LNM) compared with paired primary tissues (Fig. 1F), suggesting that increased NNT expression may promote tumorigenesis and contribute to the metastatic behavior of gastric cancer. Strikingly, Kaplan-Meier survival analysis and the log-rank test showed that NNT overexpression was correlated with poor overall survival and disease-free survival (Fig. 1F and G). Taken together, our results suggest that NNT is a potential prognostic biomarker and a promising target for GC treatment.

3.2. NNT suppression impairs NADPH homeostasis and accelerates GC cell death under glucose deprivation

NNT is located in the mitochondrial inner membrane. It couples the flow of protons down the electrochemical proton gradient to hydride transfer from NADH to NADP⁺ [21,22], indicating its critical role in redox homeostasis (Fig. 2A). To determine whether NNT is essential to homeostasis of NADPH pools in GC, we used the RNAi strategy to knock

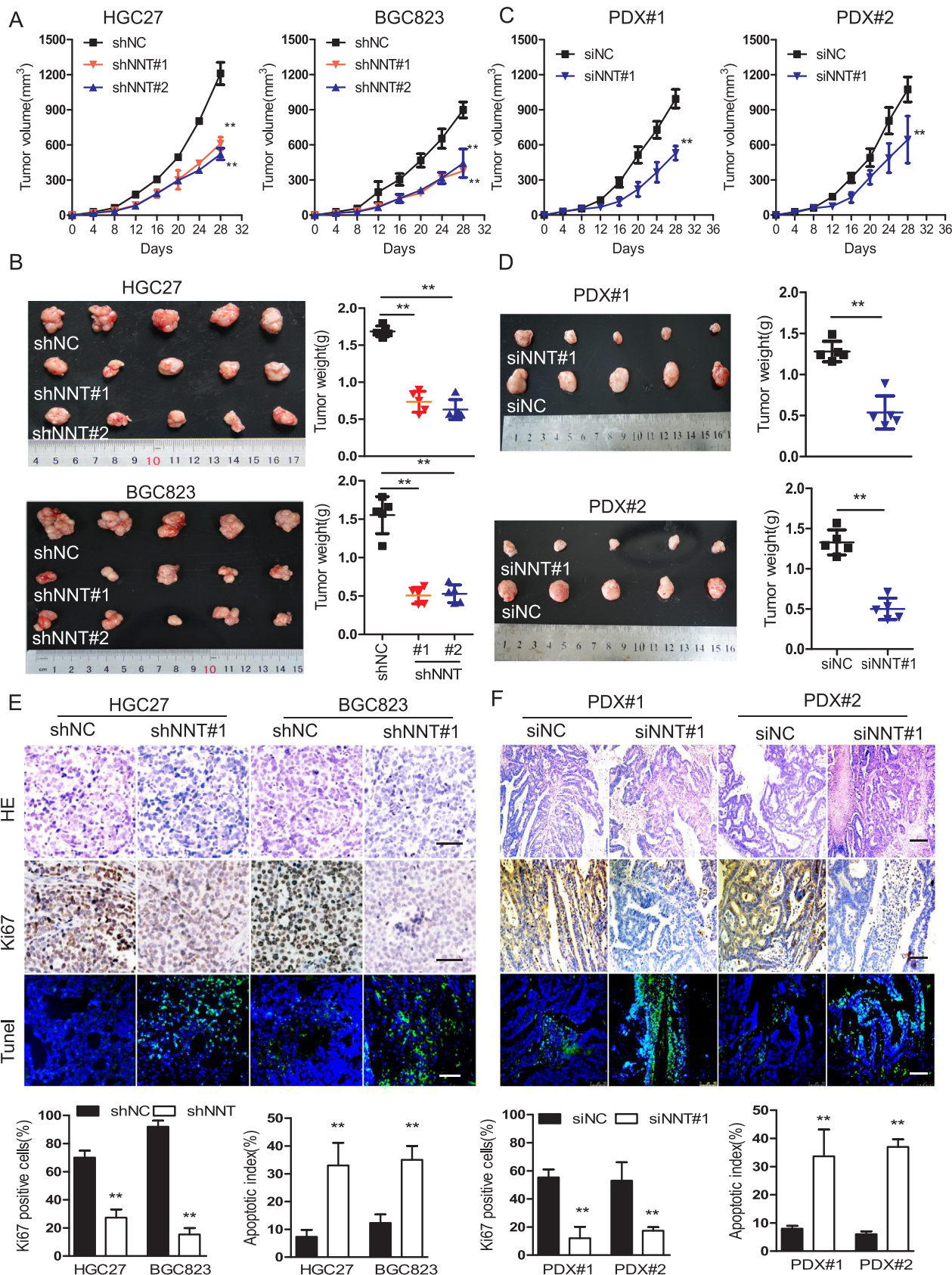
down NNT expression in HGC27 and BGC823 cells (Fig. 2B). Surprisingly, the intracellular NADPH/NADP⁺ and GSH/GSSG levels were not affected after NNT suppression in these cells (Figs. 2C, 2D, 2E). Considering that cancer cells often experience nutrition stress due to insufficient vascularization [23] and trigger the antioxidant pathway to offer protection against oxidative stress [9,24], we postulated that NNT was required for NADPH generation to maintain GSH under glucose deprivation. Thus, we cultured cells in glucose-deprivation medium to mimic the *in vivo* situation. The results indicated that the NADPH/NADP⁺ ratio was significantly decreased as well as GSH/GSSG levels in NNT-knockdown cells compared with those in control cells (Fig. 2D and E). Also, mitochondrial and cellular ROS levels were remarkably elevated after knockdown of NNT in HGC27 and BGC823 cells (Fig. 2F and G) when cultured under glucose deprivation. Indeed, further study revealed that exposure of HGC27 and BGC823 cells to glucose deprivation led to significantly elevated apoptosis after knockdown of NNT, which could be restored by pretreatment with NAC (1 mM) (Fig. 2H and I). Accordingly, NNT knockdown GC cells exhibited obvious expression of cleaved PARP and caspase 3 induced by glucose deprivation (Fig. 2J). Together, these data suggest that NNT is required for maintenance of redox homeostasis and promotion of GC cell survival during glucose deprivation.

3.3. NNT mediates anoikis resistance of gastric cancer

In addition to glucose starvation, cancer cells must adapt to and survive in the absence of the extracellular matrix during tumor metastasis [25]. We observed a significant increase in mitochondrial and cellular ROS levels in GC cells under detached conditions for 12 h (Fig. 3A and B). NNT suppression resulted in a significant decrease in NADPH/NADP⁺ as well as GSH/GSSG levels under detached conditions for 24 h (Fig. 3C and D). Further analysis revealed that cellular ROS levels were significantly increased in NNT knockdown cells under detached conditions for 12 h (Fig. 3E and F). Apoptotic assays further confirmed NNT-mediated anoikis resistance (Fig. 3G). In addition, knockdown of NNT in HGC27 and BGC823 cells significantly suppressed colonies in soft agar (Fig. 3H). These data clearly supported the notion that NNT could protect GC cells from anchorage-independent growth and enhance GC malignancy *in vitro*.

3.4. NNT inhibition suppresses GC tumorigenesis *in vivo*

To test whether NNT contributes to GC tumorigenesis *in vivo*, we performed cell-based xenograft experiments by subcutaneously injecting equal amounts of NNT knockdown or control HGC27 or BGC823 cells into BALB/c nude mice. Knockdown of NNT significantly suppressed tumor growth *in vivo* as evidenced by a slower growth curve and reduced xenograft weight (Fig. 4A and B). To further explore whether NNT could be used as a therapeutic target, we assessed the anti-tumor activity of NNT targeting siRNA in mice bearing two PDXs. The growth of tumors treated with siRNA was significantly suppressed in the PDX mice compared with the control group (Fig. 4C and D). Furthermore, biopsies on NNT knockdown HGC27 and BGC823 cells as well as PDX-induced tumors indicated reduced cell proliferation indices and enhanced cell apoptosis compared to control, as determined by Ki67 and TUNEL staining, respectively (Fig. 4E and F). Taken together,



(caption on next page)

Fig. 4. NNT inhibition suppresses GC tumorigenesis *in vivo*. (A) Tumor volume progression of subcutaneous xenografts recorded on the indicated days is shown (5 mice/group). (B) Photographs and weights of the dissected xenografts were recorded. Effect of intratumoral NNT knockdown on tumor volumes (C) and weight (D) of two PDX models (5 mice/group). (E) Paraffin-embedded tumor sections derived from the subcutaneous xenograft were stained with hematoxylin and eosin (H&E) or Ki67. Apoptotic cells were visualized by TUNEL staining (green) and counterstained with DAPI (blue). (F) H&E and immunostaining with Ki67 and TUNEL in cell line or PDX-based xenografts. Scale bars: 100 μ m. The proliferation index (Ki67 staining) and apoptotic index (TUNEL staining) in tumor sections were also quantified (lower panel). All error bars represent the S.D. of results from five mice. *P* values were determined by a two-tailed *t*-test.

these results highlight the crucial roles of NNT in promoting GC progression *in vivo*.

3.5. NNT is required for GC lung metastasis and peritoneal dissemination *in vivo*

Anchorage independence is essential for survival of cancer cells during metastasis. To analyze anoikis *in vivo*, BGC823 cells were injected into the tail vein, and then fluorescence imaging or histologic examination was used to detect lung metastasis. Mice injected with control BGC823 cells induced a heavier lung metastatic burden monitored by fluorescence imaging than NNT knockdown BGC823 cells (Fig. 5A). H&E staining of dissected lungs showed significantly more metastasis nodules in the control group compared to the knockdown groups (Fig. 5B). To further determine the effect of NNT on promoting GC peritoneal metastasis, tumor cells formed by BGC823 and HGC27 control cells or NNT knockdown cells were injected into the peritoneal cavities of mice. The results indicated that NNT suppression also significantly reduced mesenteric metastatic nodules in the intestinal wall (Figs. 5C, 5D). In addition, the mean survival times for the NNT knockdown groups in this model were longer than those in the control group of BGC823 cells (Fig. 5E). Taken together, these results highlight the crucial role of NNT in GC metastasis.

As illustrated in Fig. 5F, this study is the first to demonstrate that elevated NNT regulates GC NADPH and redox homeostasis, promotes cell survival during glucose deprivation and extracellular matrix detachment, and enhances GC tumorigenesis and metastasis.

4. Discussion

NNT is the proton-translocating inner membrane protein that catalyzes the hydride transfer between NAD^+ and NADP^+ with a key role in mitochondrial redox balance for detoxification of ROS. In humans, NNT dysfunction leads to an adrenal-specific disorder, glucocorticoid deficiency [17], macrophage inflammatory responses [26], and cardiac disease [27]. It is not known for certain if NNT suppression impairs tumor growth and metastasis. Our finding was that knockdown of NNT expression significantly reduces GC growth and metastasis under oxidative stress conditions such as glucose starvation and extracellular matrix detachment.

Cancer cells often experience nutrition stress due to excessive demand for nutrition and oxygen, as well as insufficient vascularization [23]. Tumor cells reprogram their cellular metabolism to acquire necessary nutrients and satisfy the needs of rapid cell proliferation at the expense of overproduced ROS, which requires plenty of NADPH supplementation [28–30]. NADPH plays an important role in redox defense [28]. In cancer cells, overcoming oxidative stress is a critical step for tumor progression [31]. We previously reported that disruption of G6PD resulted in a marked reduction in NADPH and enhanced sensitivity to ROS stresses in colorectal cancer [13]. In this study, we demonstrate that NNT prompts redox homeostasis through NADPH generation for overcoming oxidative stress induced by glucose deprivation, thus enhancing malignancy.

Nontransformed cells that become detached from the extracellular matrix (ECM) undergo dysregulation of redox homeostasis and cell death [6]. Cancer cells often acquire the ability to recalibrate the redox balance to survive after ECM detachment, facilitating metastatic dissemination. We then assessed whether redox regulation by NNT has a

function in anchorage-independent growth. Inhibition of NNT markedly inhibited anchorage-independent growth, which was rescued by NAC treatment. It can be envisaged that the knockdown of NNT spares NADPH, as we observed a decrease in NADPH levels in NNT-deficient cells under extracellular matrix detachment *in vitro*. Furthermore, we demonstrated that NNT suppression inhibits GC lung metastasis *in vivo*.

Peritoneal metastasis is the most frequent pattern of gastric cancer recurrence or metastasis and is a definitive determinant of prognosis. The process of peritoneal metastasis is also a type of cell detachment from the extracellular matrix. Cancer cells develop anoikis resistance due to several mechanisms including modulation of oxidative stress. However, it is not certain if NNT suppression impairs an effective peritoneal metastasis. We demonstrated that NNT suppression inhibits GC peritoneal dissemination *in vivo*. We next explored the therapeutic potential of NNT inhibition in PDX models via *in vivo* siRNA treatment. Silencing NNT significantly suppressed tumor growth and induced cell apoptosis.

5. Conclusions

Our study highlights the crucial functional roles of NNT in redox regulation and tumor progression in gastric cancer. Understanding NNT-mediated NADPH metabolism may prove useful in developing new therapies or exploring small molecules that could inhibit the activities of NNT. Inhibition of NNT may be a promising therapeutic alternative in gastric cancer treatment.

Acknowledgements

The authors thank Dr. Yun-Xin Lu (Sun Yat-sen University Cancer Center) for helpful discussion and comments.

Funding

This work was supported by the Natural Science Foundation of China (81702886, 81602137), the Natural Science Foundation of Guangdong Province (2017A030310552, 2017A030313485, 2018B030306049), the Science Technology and Innovation Foundation of Guangzhou (201607010046), the Education Department of Guangdong Province (2016KQNCX139), Foundation of Guangzhou Medical University (2014C06).

Conflict of interest

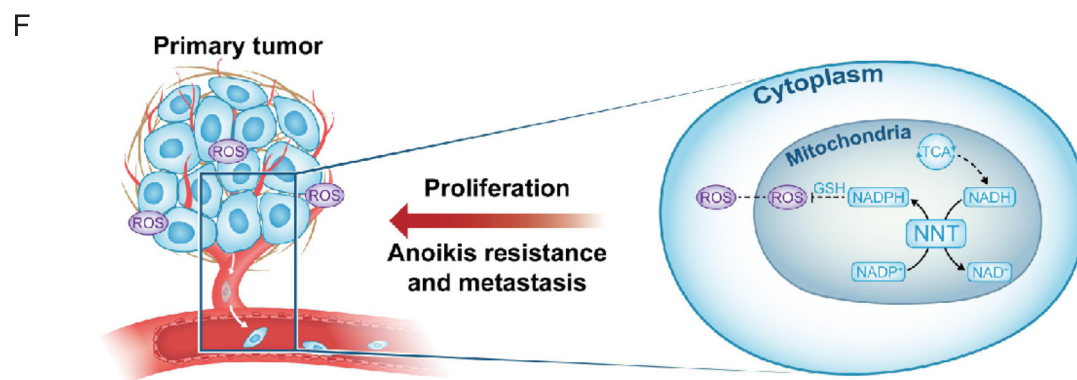
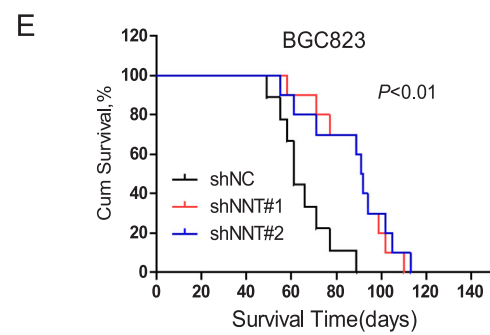
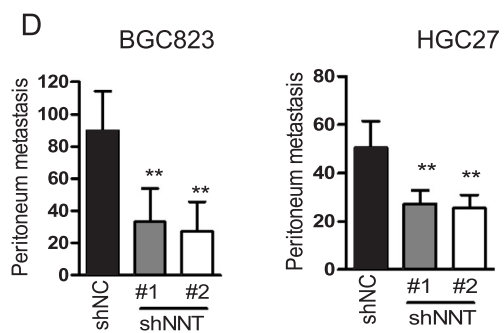
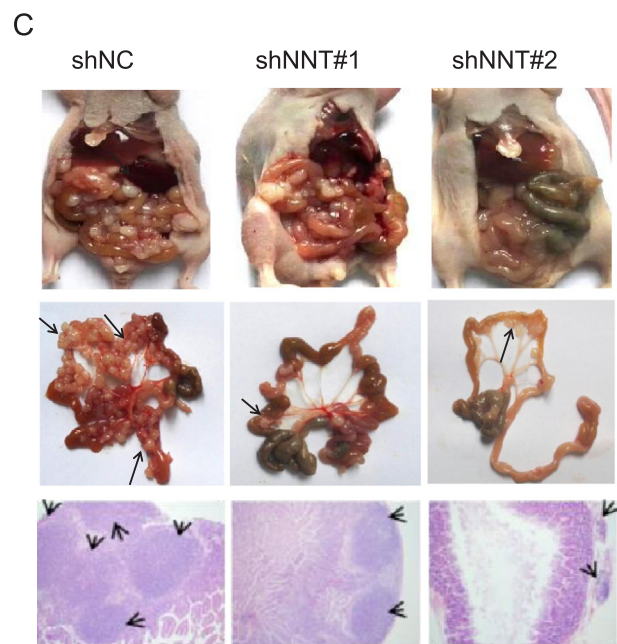
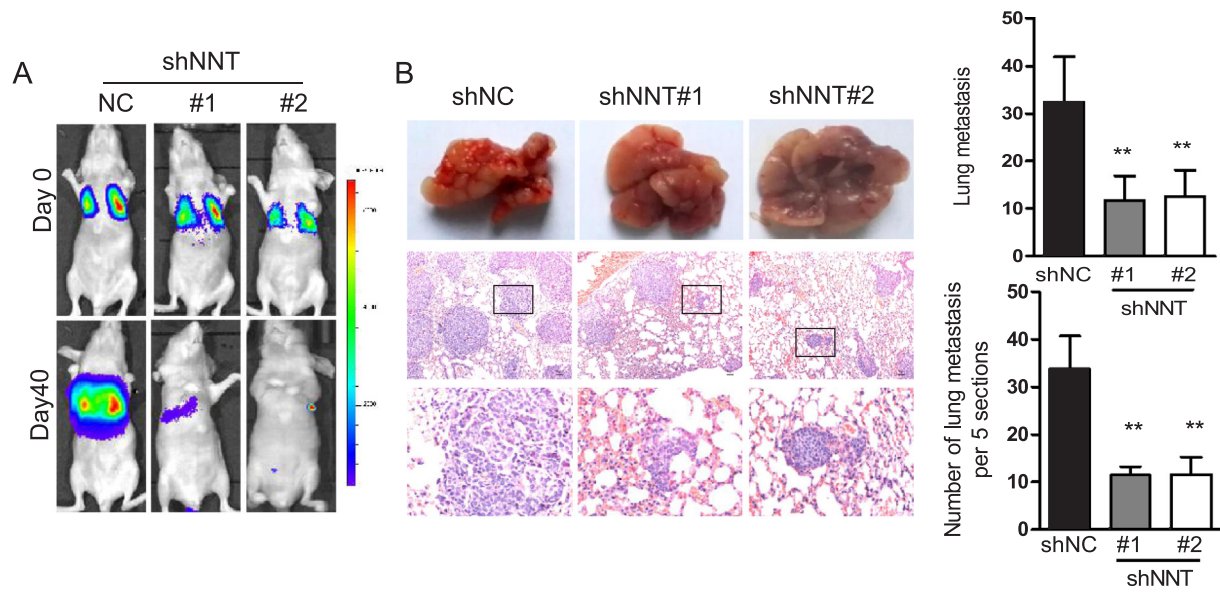
The authors disclose no conflicts.

Authors' contributions

S. Li and H.Q. Ju designed the study. S. Li, T. Wu, J. C. Lin, L.W. Deng, T. Dai, L. Lu and Z.N. Zhuang performed the *in vitro* and animal experiments. S. Li and H.Q. Ju analyzed the data. S. Li and H.Q. Ju wrote the manuscript. All authors read and approved the final manuscript.

Competing interests

The authors declare no conflict of interest.



(caption on next page)

Fig. 5. Knockdown of NNT inhibits metastasis of gastric cancer *in vivo*. Representative luciferase imaging of lung metastatic cells in nude mice after knockdown of NNT is shown. (B) Representative results of H&E staining of metastatic lung nodules from mice injected with NNT knockdown and control BGC823 cells via the tail vein for 30 days. Metastatic nodules under the naked eye or microscope were counted and recorded (right). (C–D) BGC823 and HGC27 shCon cells or shNNT cells were injected intraperitoneally, and metastases in the abdomen were recorded 30 days later (6 mice/group). Representative imaging and dissected colons were photographed, and metastatic nodules are indicated with an arrow. H&E staining of colon cells was performed, and metastatic numbers were recorded. (E) Influence of the NNT knockdown on animal survival times. Data are expressed as Kaplan-Meier survival curves (n = 10 mice per group). Survival in the NNT knockdown groups was significantly prolonged compared to the control group. (F) Proposed working model of this study. Error bars represent the S.D. of results from six mice. P values were determined by a two-tailed t-test.

Ethics approval

GC tissues were collected from patients who underwent surgical resection at the Sun Yat-sen University Cancer Center (SYSUCC, Guangzhou, China). All patients signed consent letters and all manipulation of the tissues was approved by the Ethics Committee of Sun Yat-sen University. All animal procedures were in accordance with the guidelines of the Institutional Animal Care and Use Committee and the guidelines of the Guangzhou medical University and Sun Yat-sen University.

Appendix A. Supplementary material

Supplementary data associated with this article can be found in the online version at doi:10.1016/j.redox.2018.07.017.

References

- [1] A. Jemal, M.M. Center, C. DeSantis, E.M. Ward, Global patterns of cancer incidence and mortality rates and trends, *Cancer Epidemiol. Biomark. Prev.* 19 (2010) 1893–1907.
- [2] J. Ferlay, I. Soerjomataram, R. Dikshit, S. Eser, C. Mathers, M. Rebelo, D.M. Parkin, D. Forman, F. Bray, Cancer incidence and mortality worldwide: sources, methods and major patterns in GLOBOCAN 2012, *Int. J. Cancer* 136 (2015) E359–E386.
- [3] R. Zheng, H. Zeng, S. Zhang, W. Chen, Estimates of cancer incidence and mortality in China, 2013, *Chin. J. Cancer* 36 (2017) 66.
- [4] H.H. Hartgrink, E.P. Jansen, N.C. van Grieken, C.J. van de Velde, Gastric cancer, *Lancet* 374 (2009) 477–490.
- [5] L. Yang, Z. He, J. Yao, R. Tan, Y. Zhu, Z. Li, Q. Guo, L. Wei, Regulation of AMPK-related glycolipid metabolism imbalances redox homeostasis and inhibits anchorage independent growth in human breast cancer cells, *Redox Biol.* 17 (2018) 180–191.
- [6] M.A. Hawk, Z.T. Schafer, Mechanisms of redox metabolism and cancer cell survival during extracellular matrix detachment, *J. Biol. Chem.* 293 (2018) 7531–7537.
- [7] D.C. Altieri, Mitochondria on the move: emerging paradigms of organelle trafficking in tumour plasticity and metastasis, *Br. J. Cancer* 117 (2017) 301–305.
- [8] T. Stylianopoulos, J.D. Martin, M. Snuderl, F. Mpekris, S.R. Jain, R.K. Jain, Coevolution of solid stress and interstitial fluid pressure in tumors during progression: implications for vascular collapse, *Cancer Res.* 73 (2013) 3833–3841.
- [9] S.S. Sabharwal, P.T. Schumacker, Mitochondrial ROS in cancer: initiators, amplifiers or an Achilles' heel? *Nat. Rev. Cancer* 14 (2014) 709–721.
- [10] Z.T. Schafer, A.R. Grassian, L. Song, Z. Jiang, Z. Gerhart-Hines, H.Y. Irie, S. Gao, P. Puigserver, J.S. Brugge, Antioxidant and oncogene rescue of metabolic defects caused by loss of matrix attachment, *Nature* 461 (2009) 109–113.
- [11] A.G. Nickel, A. von Hardenberg, M. Hohl, J.R. Löffler, M. Kohlhaas, J. Becker, J.C. Reil, A. Kazakov, J. Bonnekoh, M. Stadelmaier, et al., Reversal of mitochondrial transhydrogenase causes oxidative stress in heart failure, *Cell Metab.* 22 (2015) 472–484.
- [12] M.P. Murphy, Redox modulation by reversal of the mitochondrial nicotinamide nucleotide transhydrogenase, *Cell Metab.* 22 (2015) 363–365.
- [13] H.Q. Ju, Y.X. Lu, Q.N. Wu, J. Liu, Z.L. Zeng, H.Y. Mo, Y. Chen, T. Tian, Y. Wang, T.B. Kang, et al., Disrupting G6PD-mediated Redox homeostasis enhances chemosensitivity in colorectal cancer, *Oncogene* 36 (2017) 6282–6292.
- [14] Y.X. Lu, H.Q. Ju, Z.X. Liu, D.L. Chen, Y. Wang, Q. Zhao, Q.N. Wu, Z.L. Zeng, H.B. Qiu, P.S. Hu, et al., ME1 regulates NADPH homeostasis to promote gastric cancer growth and metastasis, *Cancer Res.* 78 (2018) 1972–1985.
- [15] E. Meimaridou, M. Goldsworthy, V. Chortis, E. Fragouli, P.A. Foster, W. Arlt, R. Cox, L.A. Metherell, NNT is a key regulator of adrenal redox homeostasis and steroidogenesis in male mice, *J. Endocrinol.* 236 (2018) 13–28.
- [16] H.Y. Ho, Y.T. Lin, G. Lin, P.R. Wu, M.L. Cheng, Nicotinamide nucleotide transhydrogenase (NNT) deficiency dysregulates mitochondrial retrograde signaling and impedes proliferation, *Redox Biol.* 12 (2017) 916–928.
- [17] E. Meimaridou, J. Kowalczyk, L. Guasti, C.R. Hughes, F. Wagner, P. Frommolt, P. Nurnberg, N.P. Mann, R. Banerjee, H.N. Saka, et al., Mutations in NNT encoding nicotinamide nucleotide transhydrogenase cause familial glucocorticoid deficiency, *Nat. Genet.* 44 (2012) 740–742.
- [18] S. Li, Y. Mao, T. Zhou, C. Luo, J. Xie, W. Qi, Z. Yang, J. Ma, G. Gao, X. Yang, Manganese superoxide dismutase mediates anoikis resistance and tumor metastasis in nasopharyngeal carcinoma, *Oncotarget* 7 (2016) 32408–32420.
- [19] Q.N. Wu, Y.F. Liao, Y.X. Lu, Y. Wang, J.H. Lu, Z.L. Zeng, Q.T. Huang, H. Sheng, J.P. Yun, D. Xie, et al., Pharmacological inhibition of DUSP6 suppresses gastric cancer growth and metastasis and overcomes cisplatin resistance, *Cancer Lett.* 412 (2018) 243–255.
- [20] H.Q. Ju, H. Ying, T. Tian, J. Ling, J. Fu, Y. Lu, M. Wu, L. Yang, A. Achreja, G. Chen, et al., Mutant Kras- and p16-regulated NOX4 activation overcomes metabolic checkpoints in development of pancreatic ductal adenocarcinoma, *Nat. Commun.* 8 (2017) 14437.
- [21] J.B. Jackson, J.H. Leung, C.D. Stout, L.A. Schurig-Briccio, R.B. Gennis, Review and hypothesis. New insights into the reaction mechanism of transhydrogenase: swivelling the dIII component may gate the proton channel, *FEBS Lett.* 589 (2015) 2027–2033.
- [22] A. Pedersen, G.B. Karlsson, J. Rydstrom, Proton-translocating transhydrogenase: an update of unsolved and controversial issues, *J. Bioenerg. Biomembr.* 40 (2008) 463–473.
- [23] G. Kroemer, J. Pouyssegur, Tumor cell metabolism: cancer's Achilles' heel, *Cancer Cell* 13 (2008) 472–482.
- [24] A. Raghunath, K. Sundarraj, R. Nagarajan, F. Arfuso, J. Bian, A.P. Kumar, G. Sethi, E. Perumal, Antioxidant response elements: discovery, classes, regulation and potential applications, *Redox Biol.* 17 (2018) 297–314.
- [25] C.L. Buchheit, K.J. Weigel, Z.T. Schafer, Cancer cell survival during detachment from the ECM: multiple barriers to tumour progression, *Nat. Rev. Cancer* 14 (2014) 632–641.
- [26] V.M. Ripoll, N.A. Meadows, M. Bangert, A.W. Lee, A. Kadioglu, R.D. Cox, Nicotinamide nucleotide transhydrogenase (NNT) acts as a novel modulator of macrophage inflammatory responses, *FASEB J.* 26 (2012) 3550–3562.
- [27] M.N. Bainbridge, E.E. Davis, W.Y. Choi, A. Dickson, H.R. Martinez, M. Wang, H. Dinh, D.M. Muzny, R. Pignatelli, N. Katsanis, et al., Loss of function mutations in NNT are associated with left ventricular noncompaction, *Circ. Cardiovasc. Genet.* 8 (2015) 544–552.
- [28] N.N. Pavlova, C.B. Thompson, The emerging hallmarks of cancer metabolism, *Cell Metab.* 23 (2016) 27–47.
- [29] S.M. Jeon, N.S. Chandel, N. Hay, AMPK regulates NADPH homeostasis to promote tumour cell survival during energy stress, *Nature* 485 (2012) 661–665.
- [30] A. Carracedo, L.C. Cantley, P.P. Pandolfi, Cancer metabolism: fatty acid oxidation in the limelight, *Nat. Rev. Cancer* 13 (2013) 227–232.
- [31] C. Gorrini, I.S. Harris, T.W. Mak, Modulation of oxidative stress as an anticancer strategy, *Nat. Rev. Drug Discov.* 12 (2013) 931–947.